Journal of Applied Polymer Science

Thermoplastic rubber/PP elastomers toward extremely low thermal expansion

Kun Zhang, Dongge Zhang, Lili Su, Lili Jiang, Jiandi Jiang, Guozhang Wu
Shanghai Key Laboratory of Advanced Polymeric Materials, School of Materials Science and Engineering, East China University of Science and Technology, Shanghai, 200237, China
Correspondence to: G. Wu (E-mail: wgz@ecust.edu.cn)

ABSTRACT: Fine regulation of the microstructure of rubber/polypropylene (PP) alloys could remarkably reduce the coefficient of linear thermal expansion (CLTE) while retaining the mechanical properties similar to those of thermoplastic elastomers. Rubber/PP elastomers with different morphologies were successfully prepared by controlling the appropriate rubber type, viscosity ratio, and processing method. The CLTE of the polymer alloy parallel to the microlayer directions was considerably reduced when the rubber domains were deformed into microlayers and co-continuous with plastic domains. The thickness of the PP layers played a crucial role on CLTE reduction. The CLTE considerably decreased with reduced thickness of the PP layer. The sample with a co-continuous microlayer structure exhibited good flexibility, high elongation, low hardness, and permanent deformation. Thus, low-thermal-expansion elastomer materials may have wide applications. Stress relaxation and strain recovery of the ethylene–propylene–diene terpolymer/PP (70/30 wt %) blend were investigated to further clarify the influence of co-continuous microlayer structure on mechanical properties. Anisotropic mechanical properties were consistent with the morphology. Results of the stress relaxation behavior test would provide further support to the mechanism of the low thermal expansion of blends with co-continuous microlayer structure.
 J. Appl. Polym. Sci. **2016**, *133*, 43902.

KEYWORDS: blends; elastomers; structure–property relations; thermal properties

Received 7 March 2016; accepted 5 May 2016
DOI: 10.1002/app.43902

INTRODUCTION

Heat expansion and cold contraction are basic attributes of materials. Atoms and molecules of materials maintain greater thermal motion and average separation as temperature increases, thereby increasing geometric dimension. The thermal expansion coefficient is inversely proportional to interatomic or intermolecular mutual action. Van der Waals force is considerably weaker than metal and covalent bonds. Hence, the coefficient of linear thermal expansion (CLTE) of polymers is 5–10 times higher than that of metals and 10–50 times higher than that of ceramics.[1] Stiffness generally increases with increasing bonding strength, so the thermal expansion coefficient of materials decreases with increasing strength or stiffness.[2] Hence, soft materials, such as rubber, exhibit high thermal expansion.

Reducing the CLTE of materials for engineering applications is important to achieve dimensional stability. CLTE is reduced traditionally by adding inorganic fillers with low thermal expansion, such as calcium carbonate, talc, and glass fiber.[3–7] Dalton *et al.*[8] showed that incorporating carbon nanotube ropes in a colloidal polymer film yielded a belt-like polymer. The nanotube network hindered the expansion in the plane of the film and forced an increased expansion in the out-of-plane direction. Motoc *et al.*[9] fabricated hybrid composites with zero thermal expansion. The composites were formed from various layers of glass mat and/or glass woven embedded along with layers of unidirectional carbon fibers into a polymeric matrix. However, traditional low-thermal-expansion composites have significantly high stiffness, which results in loss of rubber property. Rao *et al.*[5] studied the mechanical properties and thermal expansion behaviors of PEO-Clay composites. Though the addition of 12.5% clay reduced the thermal expansion from 11.7×10^{-5}/°C to 1.2×10^{-5}/°C, the break elongation reduced from 60% to 1% and Young's modulus increased from 0.8 GPa to 6.2 GPa. Thus, the use of fillers to reduce thermal expansion remains significantly limited.

Rubbers can be used as additives to tune the thermal expansion behavior of semi-crystalline polymers to fabricate polymer blends with very low CLTE.[10,11] Deformation of rubber and plastic domains into microlayers considerably reduce the CLTEs

Additional Supporting Information may be found in the online version of this article.

of polymer blends parallel to the direction of the microlayers. Ono *et al.*[12,13] and Kim *et al.*[14] observed a similar phenomenon in polypropylene (PP)/elastomer systems. Consequently, controlling the morphology of rubber-toughened plastics may be used to design polymer blends with desirable dimensional stability. However, the rubber contents in these studies were less than 50 wt %. The Hence, the plastic/rubber blends showed no rubber property. In the current study, a remarkable approach is proposed to design thermoplastic elastomers with very low CLTE. An immiscible plastic/rubber blend co-continuously structured with rubber content up to 70 wt % or 80 wt % was fabricated. A relatively low viscosity of plastic with strong nonlinear viscoelasticity should be beneficial for co-continuous deformation.[13,15–18] Another key factor is compatibility. Good compatibility helps control, coalescence, and improves adhesion between the two phases.[19–21] It was reported that a high viscosity of dispersed phase[13] and poor compatibility between rubber and plastic[20] led to high phase size and low co-continuity.

Material deformation is significantly relevant to practical engineering application. Numerous studies[22–26] have investigated the relationship between the three-dimensional anisotropy of a microstructure and mechanical properties. Mechanical properties can significantly differ in the various testing directions for tensile, compressive, and bending loading conditions.[23–27] Lesser *et al.*[28] investigated the correlation between orientation and stress relaxation time of pre-stressed competitive double-network elastomeric systems. The time constant corresponding to the oriented structure decreased with increase in degree of orientation. However, very few studies have reported on the compressive behavior of polymer blends with co-continuous microlayer structure. Thus, this article addresses some issues on these polymers.

The effect of compatibility and viscosity ratio on the structure of rubber/plastic blends was investigated. Moreover, the correlation between the structure and thermal expansion behavior was analyzed. Poly(ethylene-*co*-octene) (EOR), ethylene-propylene-diene monomer (EPDM), and ethylene–propylene rubber (EPR) were each compounded with PP using a two-screw extruder and then subjected to injection molding. The correlation between morphologies and mechanical properties of EPDM/PP blends with co-continuous microlayer structure was also investigated.

EXPERIMENTAL

Raw Materials and Sample Preparation

Table I summarizes the materials used in this study. Binary blends were mixed with a twin-screw extruder (KS-2, L/D = 44; Kunshan, China). The extrudate was continuously cooled in a water trough, air dried, and then pelletized prior to injection molding. Then, the mixture was subjected to injection molding (HTF86/TJ, China) and hot-pressed at 240 °C. The schematic diagram of injection-molded sample is shown in Figure 1. Prior to the tests, the specimens were placed in vacuum desiccators for 4–6 days at 23 °C immediately after molding. EPDM/PP thermoplastic vulcanizate was prepared as previously described.[29] The specimens were annealed at 120 °C for 4 h before the test to eliminate thermal history and residual stress.

Table I. Materials Used

Reference	Grade name	Viscosity[a] (Pa s)	Supplier
PP-L	H39S-2	280	Dalian Petrochemical Co.
PP-H	S1003	650	SECCO
EOR-L	Engage8407	200	Dow
EOR-H	Engage8130	420	Dow
EPDM	V5601	3400	ExxonMobil
EPR	EP02P	2000	JSR

[a] The shear rate was 50 rad/s at 240 °C.

Morphological Observations

The injection-molded specimens for morphological observations were cut from the area with grids shown in Figure 1. Transmission electron microscopy (HT7700, Hitachi) was conducted. Ultra-thin sections approximately 60 nm thick were cryogenically cut by a diamond knife. Sections were collected on holey grids and then stained with OsO_4 vapor to enhance the phase contrast between PP and rubbers. Specimens for scanning electron microscopy (S-4800, Hitachi) were etched with n-heptane to remove EPDM and then fractured in liquid nitrogen. The fractured surface was coated with gold and then morphologically observed at an accelerating voltage of 5 kV. Quantitative image analysis was performed by a digital file in Adobe Photoshop.

Thermal Expansion Measurements

CLTE was measured in accordance with ASTM E831 standards using a thermomechanical analyzer (DMA2980, TA instrument, USA) in penetration mode. Rectangular specimens were prepared from the grid region with the following dimensions: 8 mm length [flow direction (FD)] × 6 mm width [transverse direction (TD)] × 3 mm thickness [normal direction (ND)] (Figure 1). The specimens were annealed at 120 °C for 4 h before the test to eliminate thermal history and residual stress. The average value of CLTE from −35 °C to 45 °C was calculated.

Mechanical Properties

The stress–strain properties of the specimens were measured using a universal material testing machine in tensile mode (SANS CMT-4000, New Sansi Group) and a dynamic

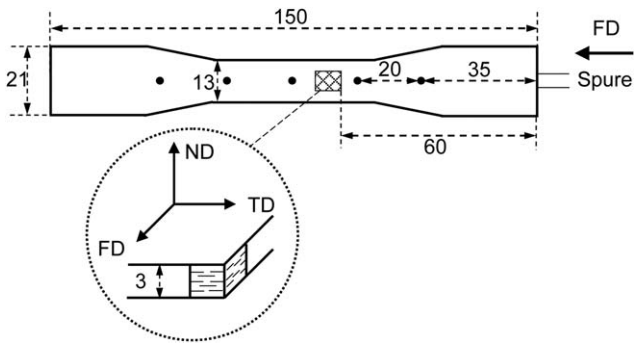

Figure 1. Schematic diagram of injection-molded sample and cut specimens (thickness =3 mm).

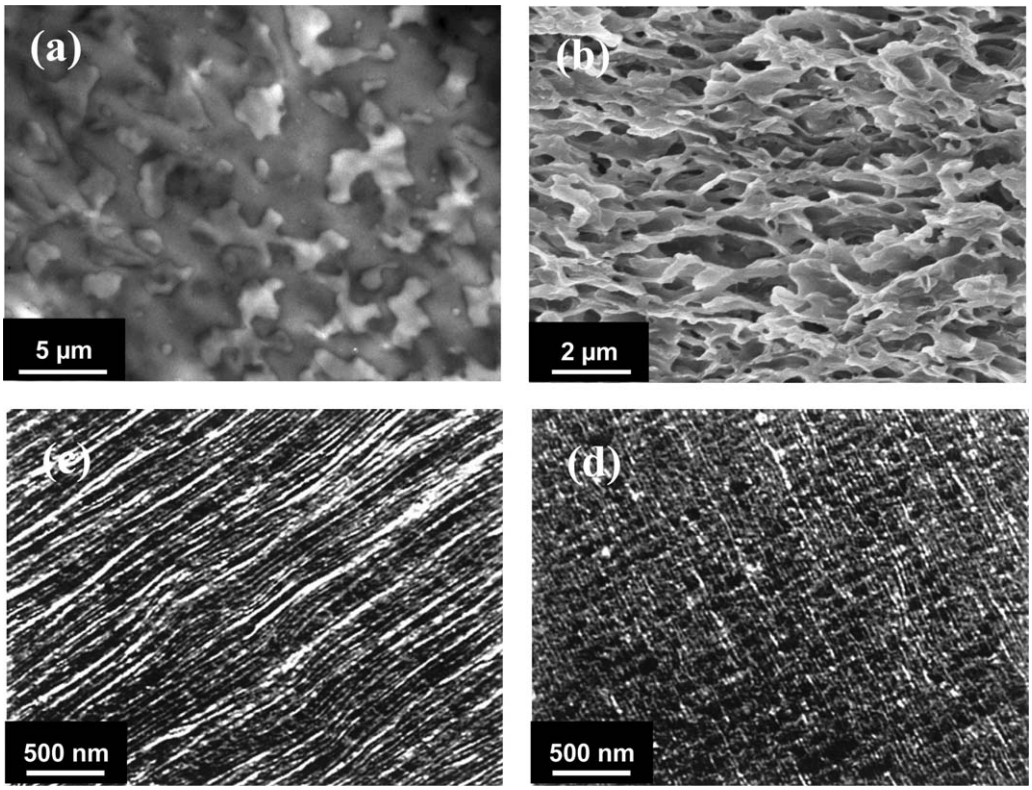

Figure 2. Morphology of PP mixtures with different rubber concentrations. (a) Transmission electron micrograph of the press-molded EPDM-70-0.19 sheet; (b) scanning electron micrograph of the injection-molded EPDM-70-0.19 sheet in the flow direction (FD); and transmission electron micrographs of the injection-molded (c) EPR-60-0.14 and (d) EPR-80-0.14 sheets in FD.

mechanical analyzer (DMA2980) in compression mode. The specimens were subjected to tensile test at a head displacement rate of 50 mm/min at room temperature. The specimens for compressive test were cut into cubes with 3 mm sides in the same region for the thermal expansion test (Figure 1). The specimens for stress relaxation were held at 80 °C, 100 °C, and 120 °C for 30 min. Then, the specimens sustained an instantly imposed 10% relative strain (strain rate > 500%/min) for 10,000 s, followed by a strain recovery period of 10,000 s with a contact force of 0.001 N. Hardness was tested on five black points as shown in Figure 1. The hardness listed was the average value from five specimens.

RESULTS AND DISCUSSION

Morphology of PP/Rubber Blends

In this article, X-Y-Z denotes the following: X, rubber type; Y, rubber concentration; and Z, viscosity ratio of PP to rubber. Thus, EPDM-70-0.19 means that PP is mixed with 70 wt % EPDM and their viscosity ratio is 0.19. EPDM-70-V is a dynamic vulcanized sample containing 70 wt % EPDM. Figure 2 shows the morphologies of the rubber/PP blends. The dark areas in the transmission electron micrographs represent the rubber domains. An incomplete co-continuous structure was found in the press-molded EPDM-70-0.19 blend [Figure 2(a)].[30] Both plastic and rubber phases were elongated and oriented along the FD in the injection-molded EPDM/PP and EPR/PP blends [Figures 2(b–d)]. The scanning electron micrograph shows the co-continuous microlayer structure of injection-molded EPDM-70-0.19 blend. A similar structure was observed in EOR/PP blends with different viscosity ratios as shown in Supporting Information Figure S1. A fine co-continuous microlayer structure was observed in EPR-60-0.14 blend. However, the oriented PP domains in EPR-80-0.14 blend were separated and dispersed in EPDM domains. According to the theory of Paul and Barlow, the low content component in blends tends to disperse in the high content component.[31] The microscopic images indicate that the critical rubber content of rubber/PP blends with co-continuous microlayer structure was 70 wt %. When the rubber content was higher than 70 wt %, the co-continuous PP domains evolved to disperse phase in the continuous rubber phase.

The compatibility between rubber and plastic[20] and their viscosity ratio[11] considerably influence the domain size and thickness of microlayers. The compatibility with PP varies in the following order: EOR > EPDM ~ EPR.[32,33] However, in this study, the domain size in EOR/PP blends was larger than those in other blends, which may be ascribed to viscosity. In general, the rheology foundation to produce polymer blend with microlayer structure is the flow of binary phase, in which melt viscosity and elasticity ratio are the most important parameters.[34] Higher viscosity of the matrix phase can delay the break-up time after shear deformation, thereby favoring lamellar orientation.[11,13] Our results are consistent with the conclusion of the published articles.

Thermal Expansion Behavior

Figure 3(a) shows a typical plot of the normalized linear expansion dL/L as a function of temperature for EPDM, PP-H, press-molded, and injection-molded EPDM-70-0.19 blends in

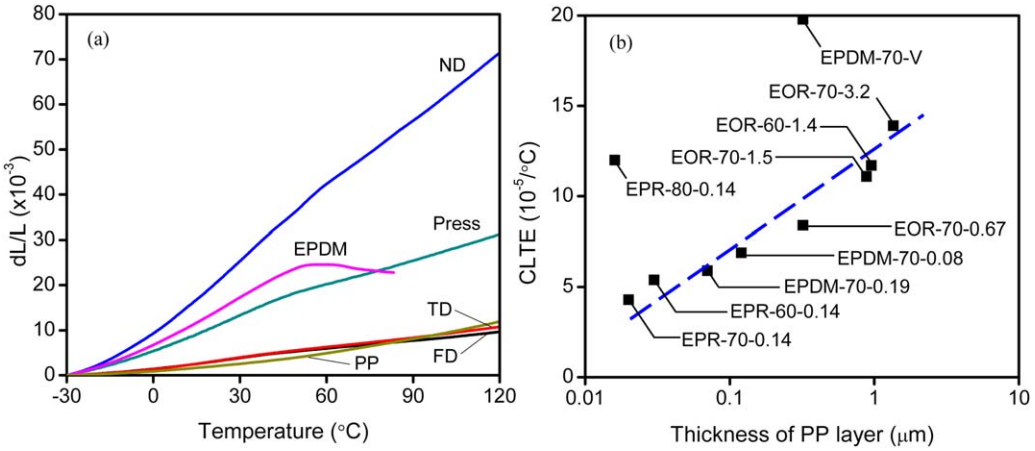

Figure 3. (a) Temperature dependence of linear expansion for injection-molded EPDM-70-0.19 mixtures in different directions (FD, TD, and ND noted as flow direction, transverse direction, and normal direction, respectively). Data for press-molded PP, EPDM, and EPDM-70-0.19 are also shown for comparison; (b) CLTE in the FD as a function of thickness of the PP layer for various injection-molded rubber/PP elastomers. [Color figure can be viewed in the online issue, which is available at wileyonlinelibrary.com.]

different directions. The press-molded sample exhibited isotropic thermal expansion.[30] Nevertheless, the injection-molded sample showed an anisotropic thermal expansion, and the thermal expansions in FD and TD were similar to that of neat PP. These results indicate that adding 30 wt % PP significantly reduced the CLTE of rubber to a value near that of PP. Furthermore, the thermal expansion in ND is higher than that of neat EPDM, which breaks the top limitation of thermal expansion for polymeric materials. The average CLTE over a temperature range from −30 °C to 45 °C was calculated by $\alpha = \frac{1}{l_1} \times \frac{l_2 - l_1}{T_2 - T_1}$, where l_1 is the length at T_1 ($T_1 = -30$ °C) and l_2 is the length at T_2 ($T_2 = 45$ °C). The average CLTEs of the injection-molded EPDM/PP blend in FD, TD, and ND were calculated to be 6.7 × 10^{-5}/°C, 6.9 × 10^{-5}/°C, and 46.3 × 10^{-5}/°C, respectively. The thermal expansions for neat PP-H, neat EPDM, and press-molded EPDM-70-0.19 (denoted as Press) were isotropic, and their CLTEs were 5.2 × 10^{-5}/°C, 30.0 × 10^{-5}/°C, and 21.0 × 10^{-5}/°C, respectively. The bulk expansion coefficient was 59.9 × 10^{-5}/°C for the press-molded sample and 63.0 × 10^{-5}/°C for the injection-molded one. This coefficient was calculated by adding the linear coefficients in the three directions. Injection molding did not significantly change the bulk expansion coefficient. Moreover, the great reduction in the CLTE in FD and TD for the injection-molded blend occurred because of the high expansion in the ND.

An image analysis software was used to determine the average thickness of the layers. Figure 3(b) presents the CLTE in FD as a function of the thickness of PP microlayers which was determined from the micrographs. Figure 3(b) clearly shows that the CLTE of the injection-molded PP/rubber blends decreased linearly with decreasing thickness of PP layers. The CLTE was reduced from 13.9 × 10^{-5}/°C (EOR-70-3.2) to 4.3 × 10^{-5}/°C (EPR-70-0.14) with PP thickness reduction from 1.35 μm (EOR-70-3.2) to 0.02 μm (EPR-70-0.14). The injection-molded EPR-70-0.14 exhibited an extremely low CLTE.

The PP thickness plays a crucial role in CLTE reduction. The large reduction in CLTE should originate from the high-order microstructure in two aspects: (1) the rubber-deformation-induced orientation of PP crystalline in which the *c*-axis with the lowest CLTE orients along FD, and (2) the co-continuous orientation of the rubber and plastic nanolayers, the thermal expansion of which favors the ND.[10,13] Yamada *et al.*[35] reported that the CLTE of PP crystalline along the *b*-axis was 2.6-fold greater than that along the *a*-axis, and the CLTE along the *c*-axis was about 10% of the *a*-axis. Reducing the PP microlayer thickness helped enhance the aspect ratio of domains and the orientation of PP crystalline,[12,36] which is beneficial in reducing the CLTE. The orientation states and co-continuity are complex in the injection-molded system, which may lead to fluctuant values of CLTE. Interfacial compatibility plays a significant role in lowering the phase size because adequate interfacial force is beneficial for the deformation of the dispersed phase.[20,37,38] The effects of viscosity ratio and compatibility between rubber and plastic could be represented by the microlayer thickness. Controlling the viscosity ratio and compatibility is necessary to reduce CLTE.

Figure 3(b) also shows two exceptions. First case is the injection-molded EPR-80-0.14, in which only 20 wt % PP is loaded. Compared with EPR-70-0.14, the CLTE of EPR-80-0.14 increased from 4.3 × 10^{-5}/°C to 12.0 × 10^{-5}/°C despite the reduction in the PP thickness from 0.02 μm to 0.016 μm. The transmission electron micrographs in Figure 2(d) show that the PP microlayers were very fine but were discontinuous because of the low concentration of PP. This exception implies that formation of a continuous PP microlayer is essential to reduce the CLTE. Another exception is the injection-molded EPDM-70-V. This polymer was prepared by a dynamic vulcanizing process in which the rubber cross-linked during complexation with PP, and the EPDM domains were dispersed in the PP matrix although the blend contained 70 wt % EPDM. During injection molding, the PP matrix was formed with low thickness. However, the cross-linked EPDM domain was slightly oriented along the FD and separated by the PP layer as shown in Supporting Information Figures S1(g,h). The injection-molded EPDM-70-V

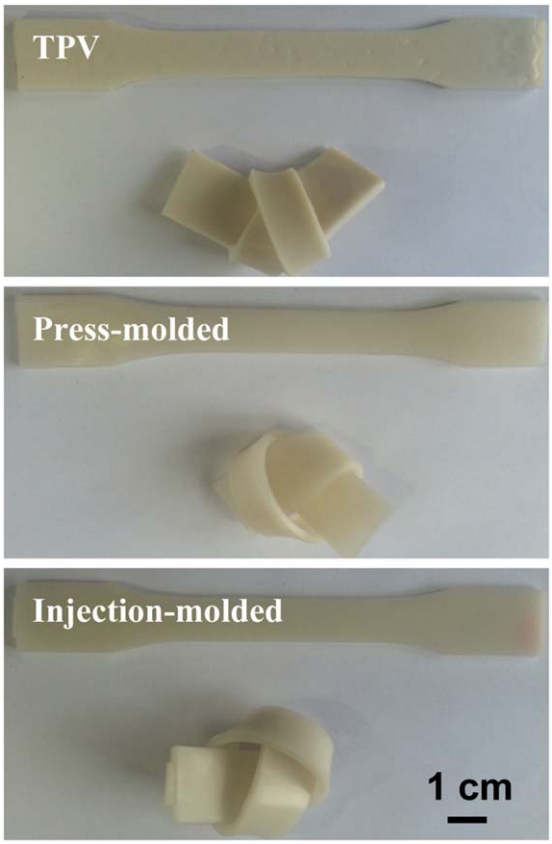

Figure 4. Sample flexibility of press-molded EPDM-70-V and EPDM-70-0.19 as well as injection-molded EPDM-70-0.19. [Color figure can be viewed in the online issue, which is available at wileyonlinelibrary.com.]

had a CLTE of 19.8 × 10^{-5}/°C, which was near that of the press-molded EPDM-70-0.19. These results clearly demonstrate the key role of co-continuous microlayer structure on lowering thermal expansion.

Rubber Characteristics of EPDM-70-0.19

Figure 4 shows the flexibility of the press-molded EPDM-70-V and EPDM-70-0.19 as well as the injection-molded EPDM-70-0.19 in different directions. These materials were prepared by the same PP and EPDM with weight ratio of 30:70. However, their microstructures are completely different. EPDM was dispersed in the PP matrix for EPDM-70-V, whereas PP was dispersed in EPDM for the press-molded EPDM-70-0.19, and a co-continuous microlayer structure for the injection-molded EPDM-70-0.19. Figure 4 shows that all samples prepared with dumbbell shape could be tied into a knot, which indicates their flexibility as elastomers.

Figure 5 shows the mechanical characteristics of the specimens. The stress–strain tension curves [Figure 5(a)] show that EPDM-70-V exhibited low elongation, and the stress almost increased linearly with the increase in strain. The press-molded and injection-molded EPDM-70-0.19 blends displayed extremely high elongation (>900%) and were not broken within the instrumental testing range. The hardness of EPDM/PP composites in ND was within the range of soft rubber (<90) according to the standard ASTM D2240. EPDM-70-V showed higher yield stress because of dynamic vulcanization.[39] Low continuity of PP domains resulted in low hardness and yield stress of press-molded EPDM-70-0.19 compared with injection-molded EPDM-70-0.19. The injection-molded EPDM-70-0.19 exhibited higher elongation and lower yield stress compared with EPDM-70-V, which should be ascribed to the lower domain size and higher continuity of EPDM.[40]

The compressibility and rebound resilience are important mechanical performance indices for elastomer materials. Figure 5(c) shows that EPDM-70-V had the highest relaxation stress under compressive test because the PP acted as the matrix and EPDM was vulcanized. Figure 5(d) shows the strain recovery following stress relaxation. Though the stress of injection-molded EPDM-70-0.19 in ND at end of the experiment time was lower than that of EPDM-70-V, the strain recovery of injection-molded EPDM-70-0.19 in ND was similar to that of EPDM-70-V. Both PP and EPDM did not show such great strain recovery. The co-continuous structure played a predominant role on the macroscopic elasticity.[41] The strain recovery of press-molded EPDM-70-0.19 was lowest because of the low co-continuity. EPDM-70-0.19 showed similar strain recovery behavior at different temperatures (80 °C, 100 °C, and 120 °C). The injection-molded sample with co-continuous microlayer structure exhibited good flexibility, high elongation, low hardness, and permanent deformation. The results provided a scientific basis for the preparation of new elastomer materials with extremely low thermal expansion. Hence, injection-molded samples treated through radiation crosslinking would exhibit low thermal expansion and high elasticity.

Anisotropic Stress Relaxation in Injection-Molded EPDM-70-0.19

Stress relaxation and strain recovery of the injection-molded and press-molded EPDM-70-0.19 were studied at different temperatures to further clarify the connection of the co-continuous microlayer structure on the mechanical properties. Figure 6 shows the stress relaxation behavior of press-molded and injection-molded EPDM-70-0.19 in different directions at 80 °C, 100 °C, and 120 °C. The injection-molded EPDM-70-0.19 exhibited an anisotropic stress relaxation. The relaxation stress shows the following trend: ND > FD > TD. The relaxation stress was reduced with increase in temperature. Anisotropic mechanical properties could also be observed in the composites with layered[27] and oriented structures.[42] The co-continuous microlayer structure is a more complex system.

The stress relaxation data were analyzed using the procedure X reported by Tobolsky *et al.*[43] The stress relaxation of EPDM-70-0.19 could be expressed as a discrete distribution, as follows:

$$\sigma(t) = \sum_{i=1}^{n} \sigma_i(0) \exp\left(-\frac{t}{\tau_i}\right) \quad (1)$$

where t is time, and $\sigma(t)$ and $\sigma(0)$ are the stresses at $t = t$ and $t = 0$, respectively. n is the number of relaxation process. τ_n are time constants for relaxation processes. The plot of $\ln[\sigma(t)]$ versus t should approach a straight line for $t > \tau_n$, if a maximum relaxation time truly exists. The intercept of the line is $\ln[\sigma_n(0)]$, and the slope is $-1/\tau_n$. Equation (1) can be written as follows:

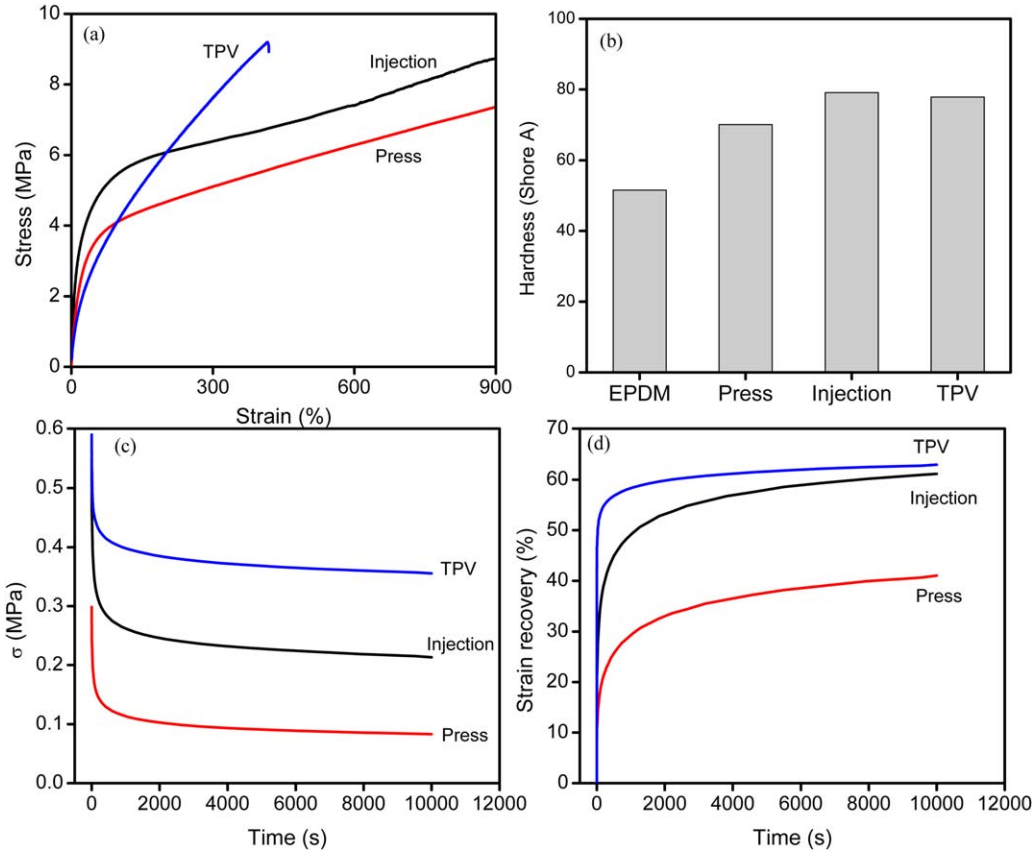

Figure 5. Mechanical characteristics of EPDM-70-V (denoted as TPV) and EPDM-70-0.19 (denoted as press molding) as well as injection-molded EPDM-70-0.19 in FD, TD, and ND directions. (a) Stress–strain tension curves; (b) Shore A hardness in ND; press stress (c) relaxation and (d) recovery curves in ND at 80 °C. [Color figure can be viewed in the online issue, which is available at wileyonlinelibrary.com.]

$$\sigma(t)-\sigma_n(0)\exp\left(-\frac{t}{\tau_n}\right)=\sum_{i=1}^{n-1}\sigma_i(0)\exp\left(-\frac{t}{\tau_i}\right) \qquad (2)$$

A slope of $\ln(\sigma(t)-\sigma_n(0)\exp(-\frac{t}{\tau_n}))$ versus t should also lead to a straight line for $t>\tau_{n-1}$, if a discrete relaxation time exists for $\tau_{n-1}<t<\tau_n$. The process can be repeated for $i=n-2$, etc., following the determination of the slope and the intercept discussed above for EPDM/PP blends $n=3$. This system is referred to as styrene–butadiene–styrene (SBS) triblock system.[28] Hence, the time constants τ_1, τ_2, and τ_3 correspond to three processes causing stress relaxation. Additionally, $\tau_1<\tau_2<\tau_3$.[28,43] The typical procedure for press-molded and injection-molded EPDM-70-0.19 in different directions at 80 °C is shown in Supporting Information Figure S3. The time constants τ_1 and τ_3 in different directions for press-molded and injection-molded EPDM-70-0.19, as well as the relaxation time of PP and EPDM, are listed in Table II. The time constants τ_1 and τ_3 were a good fit for the data of EPDM and PP, respectively. The time constants τ_1 and τ_3 are attributed to the relaxation of EPDM and PP, respectively, and they are independent of the structure of the blends.

The time constants τ_2 were plotted with respect to temperature as shown in Figure 7. The relaxation time of press-molded and injection-molded EPDM-70-0.19 decreased with increased temperature. The relaxation time of press-molded EPDM-70-0.19 was larger than that of injection-molded EPDM-70-0.19. The injection-molded EPDM-70-0.19 in different directions showed different relaxation times at the same strain as follows: $\tau_{2-ND}<\tau_{2-FD}<\tau_{2-TD}$. At high temperature, the EPDM phase lost mechanical strength, and the mechanical properties of blends were mainly provided by the PP phase, which decreased the effect of structure on the performance. Thus, the variations in relaxation time in the different directions decreased with increased temperature.

The orientation state in FD [Figure 2(b) and Supporting Information Figure S2] was higher than that in TD leading to lower relaxation stress in TD.[42] Comparison of the time constants τ_2 of press-molded and injection-molded samples in FD and TD showed a decrease in τ_2 with an increase in the orientation of morphology. Lesser *et al.*[28] reported similar results in an SBS triblock copolymer system with a double network of elastomers and associated the time constant τ_2 with the oriented network structure. Carbon nanotube composites[44–46] show similar mechanical properties. The compressive behavior shows that deformation in FD was more difficult than that in TD. The deformation in ND was more uniform.[27,42] Thus, the lowest time constant τ_2 was found in ND. The results are in accordance with the thermal expansion behavior of injection-molded sample, that is, the CLTE in FD is lower than that in TD.

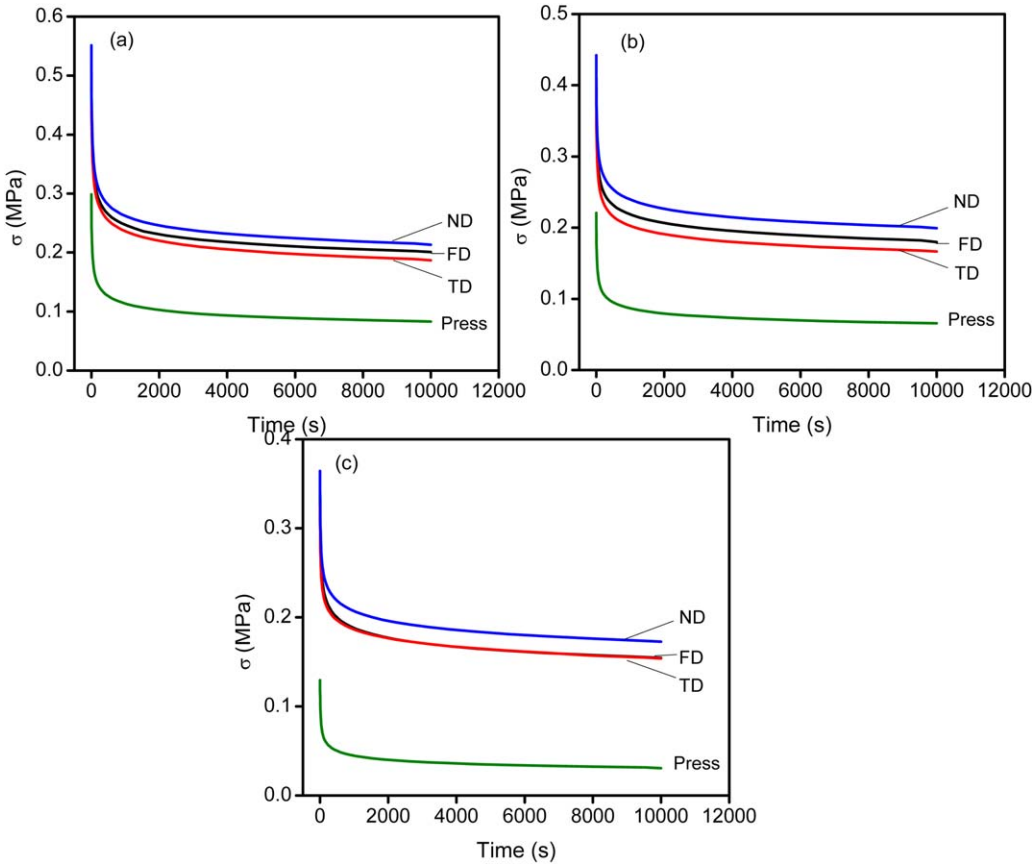

Figure 6. Stress relaxations of press-molded and injection-molded EPDM-70-0.19 during the 10,000 s of compression in different directions: (a) 100 °C and (b) 120 °C. [Color figure can be viewed in the online issue, which is available at wileyonlinelibrary.com.]

Semi-crystalline polymer/rubber blends with a co-continuous microlayer structure was previously found to exhibit an anisotropic thermal expansion behavior and the CLTE decreased with increase in orientation state of morphology.[30] The anisotropic thermal expansion behavior and mechanical properties were both caused by the co-continuous microlayer structure. Investigating the mechanical properties would provide further support to the mechanism of the low thermal expansion of blends with co-continuous microlayer structure.

Table II. Time Constants τ_1 and τ_3 in Different Directions for Press-Molded and Injection-Molded EPDM-70-0.19 and Relaxation Time of PP and EPDM

	Relaxation time (s)		
Sample	80 °C	100 °C	120 °C
τ-EPDM	32.1	30.4	30.2
τ_1-FD	26.9	23.4	20.4
τ_1-TD	26.9	25.8	24.0
τ_1-ND	25.1	21.0	19.8
τ_1-Press	27.0	25.7	23.4
τ-PP	10.1×10^4	9.5×10^4	9.2×10^4
τ_3-FD	7.3×10^4	6.9×10^4	6.5×10^4
τ_3-TD	7.4×10^4	6.9×10^4	6.4×10^4
τ_3-ND	7.3×10^4	6.9×10^4	6.5×10^4
τ_3-Press	7.2×10^4	6.9×10^4	6.5×10^4

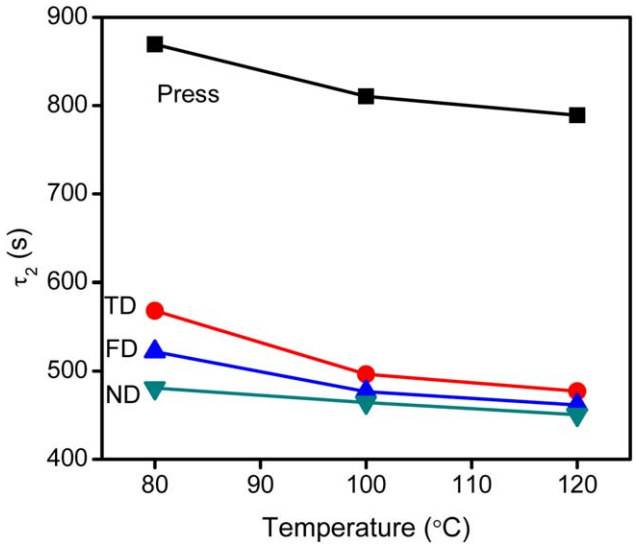

Figure 7. Temperature dependence of the time constant τ_2 in different directions for the press-molded and injection-molded EPDM-70-0.19. [Color figure can be viewed in the online issue, which is available at wileyonlinelibrary.com.]

CONCLUSIONS

A novel rubber/PP elastomer with extremely low thermal expansion is developed. The large reduction in CLTE is attributed to the fine control of the micro-morphology of polymer alloy such that the expansion is preferentially toward the thickness direction. The CLTEs of blends with co-continuous microlayer structure in FD and TD are similar to that of aluminum. The thickness of the PP layers plays a crucial role on CLTE reduction. The CLTEs decrease with reduced thickness of the PP layers. The sample with co-continuous microlayer structure exhibits low thermal expansion, good flexibility, high elongation, low hardness, and permanent deformation. The stress relaxation experimental results show that the co-continuous microlayer structure leads to a difference in relaxation time corresponding to the structure in diverse directions. The results provided a scientific basis for the preparation of new low-thermal-expansion elastomer materials. The remarkable expansion along the ND could ultimately be utilized for a range of applications, such as manufacturing of sensors, switches, and actuators from macro to micro dimensions.

ACKNOWLEDGMENTS

This work was supported by grants from the "973" project (2013CB035505), the National Natural Science Foundation of China (50873033, 51373053), and the Fundamental Research Funds for the Central Universities.

REFERENCES

1. Brandrup, J.; Immergut, E. H.; Grulke, E. A.; Abe, A.; Bloch, D. R. Polymer Handbook; Wiley: New York, **1999**.
2. Barrera, G. D.; Bruno, J. A. O.; Barron, T. H. K.; Allan, N. L. *J. Phys. Condens. Matter* **2005**, *17*, R217.
3. Lee, H.; Fasulo, P. D.; Rodgers, W. R.; Paul, D. R. *Polymer* **2006**, *47*, 3528.
4. Yoon, P. J.; Fornes, T. D.; Paul, D. R. *Polymer* **2002**, *43*, 6727.
5. Rao, Y.; Blanton, T. N. *Macromolecules* **2008**, *41*, 935.
6. Fahmy, A. A.; Ragai, A. N. *J. Appl. Phys.* **1970**, *41*, 5112.
7. Yen, H. J.; Tsai, C. L.; Wang, P. H.; Lin, J. J.; Liou, G. S. *RSC Adv.* **2013**, *3*, 17048.
8. Worajittiphon, P.; Jurewicz, I.; King, A. A.; Keddie, J. L.; Dalton, A. B. *Adv. Mater.* **2010**, *22*, 5310.
9. Motoc, D. L.; Ivens, J.; Dadirlat, N. *J. Thermal Anal. Calorim.* **2012**, *112*, 1245.
10. Wu, G.; Xu, H.; Zhou, T. *Polymer* **2010**, *51*, 3560.
11. Wu, G.; Nishida, K.; Takagi, K.; Sano, H.; Yui, H. *Polymer* **2004**, *45*, 3085.
12. Ono, M.; Nakajima, K.; Nishi, T. *J. Appl. Polym. Sci.* **2008**, *107*, 2930.
13. Ono, M.; Washiyama, J.; Nakajima, K.; Nishi, T. *Polymer* **2005**, *46*, 4899.
14. Hoon Kim, D.; Fasulo, P. D.; Rodgers, W. R.; Paul, D. R. *Polymer* **2007**, *48*, 5960.
15. Tiwari, R. R.; Paul, D. R. *Polymer* **2011**, *52*, 1141.
16. Gao, C.; Zhang, S.; Han, B.; Sun, H.; Wang, G.; Jiang, Z. *RSC Adv.* **2014**, *4*, 42175.
17. Mofokeng, J. P.; Luyt, A. S. *J. Appl. Polym. Sci.* **2015**, *132*, DOI: 10.1002/app.42138.
18. Wang, X.; Zhuang, Y.; Dong, L. *J. Appl. Polym. Sci.* **2012**, *126*, 1876.
19. Pernot, H.; Baumert, M.; Court, F.; Leibler, L. *Nature Mater.* **2002**, *1*, 54.
20. Jiang, J.; Su, L.; Zhang, D.; Zhang, K.; Wu, G. *J. Appl. Polym. Sci.* **2012**, *128*, 3993.
21. Liu, X.; Meng, X.; Wu, J.; Huo, J.; Cui, L.; Zhou, Q. *RSC Adv.* **2015**, *5*, 69621.
22. Rotella, C.; Tencé-Girault, S.; Cloitre, M.; Leibler, L. *Macromolecules* **2014**, *47*, 4805.
23. Karayaka, M.; Kurath, P. *J. Eng. Mater. Technol.* **1994**, *116*, 222.
24. Kim, Y. R.; McCarthy, S. P.; Fanucci, J. P. *Polym. Compos.* **1991**, *12*, 13.
25. Tian, M.; Yin, S.; Zou, H.; Su, L.; Zhang, L. *Compos. B* **2011**, *42*, 1937.
26. Somashekar, A. A.; Bickerton, S.; Bhattacharyya, D. *Compos. A* **2012**, *43*, 1044.
27. Akil, Ö.; Yıldırım, U.; Güden, M.; Hall, I. W. *Polym. Test.* **2003**, *22*, 883.
28. Singh, N. K.; Lesser, A. J. *Macromolecules* **2011**, *44*, 1480.
29. Wang, C.; Li, C. *Mod. Plast. Process. Appl.* **2011**, *23*, 38.
30. Zhang, K.; Jiang, L.; Luo, P.; Jiang, J.; Wu, G. *Polym. Int.* **2015**, *64*, 1225.
31. Paul, D. R.; Barlow, J. W. *J. Macromol. Sci. Rev. Macromol. Chem.* **1980**, *18*, 109.
32. Babu, R.; Singha, N.; Naskar, K. *Express Polym. Lett.* **2010**, *4*, 197.
33. Jang, B.; Uhlmann, D. R.; Vander Sande, J. *J. Appl. Polym. Sci.* **1985**, *30*, 2485.
34. Rodriguez-Veloz, O.; Kamal, M. *Adv. Polym. Technol.* **1999**, *18*, 89.
35. Gu, F.; Hikosaka, M.; Toda, A.; Ghosh, S. K.; Yamazaki, S.; Arakaki, M.; Yamada, K. *Polymer* **2002**, *43*, 1473.
36. Ono, M.; Washiyama, J.; Nakajima, K.; Nishi, T. *Polym. J.* **2004**, *36*, 563.
37. Samios, C. K.; Kalfoglou, N. K. *Polymer* **1998**, *39*, 3863.
38. Svoboda, P.; Svobodova, D.; Slobodian, P.; Ougizawa, T.; Inoue, T. *Eur. Polym. J.* **2009**, *45*, 1485.
39. Vennemann, N.; Bökamp, K.; Bröker, D. *Macromol. Symp.* **2006**, 641. pp
40. Feng, W.; Isayev, A. *Polymer* **2004**, *45*, 1207.
41. Martin, G.; Barres, C.; Sonntag, P.; Garois, N.; Cassagnau, P. *Mater. Chem. Phys.* **2009**, *113*, 889.
42. Tu, Z.; Shim, V.; Lim, C. *Int. J. Solids Struct.* **2001**, *38*, 9267.
43. Tobolsky, A.; Murakami, K. *J. Polym. Sci.* **1959**, *40*, 443.
44. Kochmann, D. M.; Drugan, W. *J., J. Mech. Phys. Solids* **2009**, *57*, 1122.
45. Carey, B. J.; Patra, P. K.; Hahm, M. G.; Ajayan, P. M. *Adv. Funct. Mater.* **2013**, *23*, 3002.
46. Suhr, J.; Victor, P.; Ci, L.; Sreekala, S.; Zhang, X.; Nalamasu, O.; Ajayan, P. M. *Nat. Nano.* **2007**, *2*, 417.